International Journal of Mechanical and Civil Engineering (IJMCE)
ISSN: 2689-940X
Volume 9, Issue 1, 2026 (pp. 18-38)
www.abjournals.org

SEM-BASED MICROSTRUCTURAL ANALYSIS AND EXPERIMENTAL OPTIMIZATION OF SAWDUST ASH IN STABILIZED LATERITIC BRICKS (SLB)

Oladapo Silas Akinkunmi[a], Olofintuyi Ilesanmi Olanrewaju[a*], Oke Oluwaseyi Lanre[b], and Ogundipe Olumide Moses[b].

[a]The Federal Polytechnic, Ado Ekiti, Ekiti State, 360231, Nigeria.

[b]Ekiti State University, Ado Ekiti, Civil Engineering Department, 360001, Nigeria.

[*]Corresponding Author's Email: olofintuyi_io@fedpolyado.edu.ng

Cite this article:

Oladapo, S. A., Olofintuyi, I. O., Oke, O. L., Ogundipe, O. M. (2026), SEM-Based Microstructural Analysis and Experimental Optimization of Sawdust Ash in Stabilized Lateritic Bricks (SLB). International Journal of Mechanical and Civil Engineering 9(1), 18-38. DOI: 10.52589/IJMCE-VWINHURC

Manuscript History

Received: 18 Mar 2026

Accepted: 20 Apr 2026

Published: 21 May 2026

ABSTRACT: *This study examines the compressed lateritic brick stabilizer sawdust ash (SDA) optimization and microstructural evaluation. In the experiment, Response Surface Methodology's Box Behnken Design (BBD) was employed. Following air drying and pulverization, lateritic soil was combined with water, cement, and pozzolan (SDA). Pouring the slurry into a hydraulic brick mould produced stabilized interlocking lateritic bricks. Compressive strength, water absorption, abrasion, impact, and sulphate attack was evaluated at 28, 56, 108, and 365 days for membrane-cured bricks. The microstructure of the bricks was also examined using an SEM. As curing ages progressed, SDA's increasing silica oxide content, calcium, alumina, and ferric oxides made it a superior pozzolan with improved compressive strength, resistance to water absorption, abrasion, impact, and sulphate. Based on optimization results, the following properties are obtained at 365 days: 5.186 N/mm² compressive strength, 6.106% water absorption, 4.067% abrasion resistance, 8.598% impact resistance, and 9.853% sulphate attack resistance: 4.571% SDA, 4.7% cement, and 25.00% water content. The optimal mix demonstrated durability by having a compressive strength that was higher than load-bearing brick standards and a decreased water absorption rate. Particle bonding, pore closure, and pozzolanic activity were all enhanced in SEM micrographs at optimal SDA levels. Based on the data, SDA can be a cost-effective and environmentally friendly stabilizing agent for waste management and construction.*

KEYWORDS: Sawdust Ash; Lateritic bricks; Optimization; Air layer; Compressive strength; Microstructure.

INTRODUCTION

To provide enough housing for the world's rising population, especially in developing countries, it is important to have access to affordable building materials. There is a growing necessity to source local materials for constructing affordable housing in both rural and urban regions as expenses persist in escalating [1]. For the creation of concrete, the building industry mostly uses traditional ingredients like cement, granite, and sand. The rising cost of these materials has made it much harder to build homes and other infrastructure in Nigeria and other developing countries. The expense of construction materials has been recognized as a major obstacle to effective housing provision [2-4]. An engineering assessment is essential for employing cost-effective and locally available materials to enhance self-sufficiency and attain a significant reduction in construction costs for sustainable development [5,6]. A decrease in material costs will undoubtedly result in significant savings in total building production expenses, as materials account for two-thirds of the whole cost [7]. Cement constitutes approximately 42% of construction expenses, and demand has markedly increased due to the current construction surge [8-10].

Cement is produced in large amounts globally due to its extensive use in concrete. Approximately 5 billion tons of cement are produced globally each year. About 600 kg-900 kg of carbon dioxide ($CO2$) is released for every 1 ton of cement produced, which has an adverse effect on the environment [11]. Research into industrial and agricultural by-products as potential alternatives has been prompted by the expectation that the growing demand for cement will be partially satisfied by way of partial substitution. The search for alternative binders or cement substitutes recognized the potential of using agricultural and industrial waste as cementitious materials. The resulting concrete has technical advantages and can replace more cement in each volume if these fillers have pozzolanic properties [12-14]. One type of agricultural and industrial residue with a lot of promise is sawdust. One recognized agricultural by-product that comes from the lumber sector is sawdust. It is produced as a by-product when timber is mechanically processed into a variety of sizes and forms. Various environmental difficulties result from sawdust waste, with the paucity of landfill space emerging as a key worry and a serious danger to developing countries.

The amount of additional sawdust garbage that is collected each year from households, businesses, and mills is increasing. In the US, Germany, the UK, and Australia, respectively, approximately 64, 8.8, 4.6, and 4.5 million tons of wood waste are produced each year; more than 40% of these volumes remain unprocessed. Inadequate recycling processes and procedures are indicated by the substantial amount of wood waste that is not recycled. Using wood fuel to generate electricity is the best solution to address the problems related to wood waste. Although thermal combustion often results in less wood waste, it also produces sawdust ash, sometimes known as wood ash. The United States produces roughly 3 million tons of wood ash annually. Tiny boiler units are often used in the timber industry to generate thermal energy for auxiliary processes like drying finished goods by burning processed wood waste as fuel. To ensure its environmentally sustainable disposal, wood waste must be recycled every day and successfully mixed into cement-based composites and concretes. Given that cement is the primary component of concrete, substituting it with ash produced from sawdust is projected to deliver various benefits, including reduced pollution, increased waste utilization, and a significant reduction in long-term building costs [20–22]. Several studies have investigated the utilization of sawdust ash for improving soil conditions in engineering applications [23-25].

Article DOI: 10.52589/IJMCE-VWINHURC
DOI URL: https://doi.org/10.52589/IJMCE-VWINHURC

Their research revealed that sawdust ash has tremendous promise as a viable substitute for cement at various optimum levels. Numerous scholars have recently engaged on sawdust optimization. One study, by [4], used the Extreme Vertex Design Method to optimize a two-component restricted simplex mixture in order to analyze the mechanical strength features of the produced green concrete.

Component restrictions were established within a range of 0% to 50% replacement of industrial waste derivatives (SDA) as supplemental cementitious material (SCM) to ascertain the ideal mixture proportion for enhanced strength response. Table 1 shows even more research studies on Saw Dust Ash from 2021 until now.

Table 1: Scopus indexed publications on compressed stabilized bricks (2019-2025)

Citation	**Material components**	**Replacement Range**	**Optimum dosage/ percentage**	**Testing**	**Motivation**	**Product**	**Location**
[21]	Cement+Stonedust+ wheat straw	10-30% Stonedust, 0.5%-1.5%Wheatstraw	20% stone dust and 0.5% wheat dust	Masonry wallet test, masonry prism test, Unit block test	Use of Wheat dust as admixture	Compressed solid bricks	China
[29]	RHA and SDA	0%-6% RHA and SDA	2%SDA+2%RHA	Compaction, Water absorption strength and SEM	Use of Rice Husk Ash and Saw Dust Ash	Compressed solid bricks	Nigeria
[28]	Stone dust (SD) and SDA	10% -30% SDA and SD	4% SDA and 20% SD	CBR and physical properties	Use of SDA to improve soil properties	Improvement of weak soil	India
[27]	Fly ash, Rice Husk Ash and Marble Dust Powder	70% to 85% Fly Ash, 15% to 30% SDA, 5% to 30%, Marble dust Powder	80% FA, 15% RHA, and 15% MDP	Compressive strength, Water absorption test and Efflorescent test	Utilization of SDA as pozzolan in geopolymer bricks	Production of geopolymer bricks	India

Article DOI: 10.52589/IJMCE-VWINHURC
DOI URL: https://doi.org/10.52589/IJMCE-VWINHURC

[26]	Saw Dust and Brick Ballast	4%, 8% and 12% Saw Dust (SD) and 8%, 16% and 24% Brick Ballast (BB)	4% of sawdust and 24% of Brick ballast	Compressive strength, Index properties	Utilization saw dust in light weight concrete	Production of light weight concrete production	India
[12]	Rice straw Ash	2%, 4%, 6%, 8%, and 10% of Rice Straw Ash	2% and 4% ash	XRD, Compressive strength	The mechanical, durability, and microstructural properties of clay bricks made from rice, straw, and ash	Making clay bricks with ash from rice straw	India
[15]	Saw Dust Ash	(5, 10, and 15 wt.%)	10% SDA	Split Tensile test, compressive strength and compressive strength	Partial replacement of cement with SDA in concrete	Production of concrete bricks with SDA .	Turkey
[25]	Saw Dust Ash and cement	Ratio of 875:0.125 SDA:Cement	0.89: 0.11 SDA:Cement	Development of model	Components generation and development of ANOVA	Utilizations of Extreme Vertex Design method	Nigeria

Article DOI: 10.52589/IJMCE-VWINHURC
DOI URL: https://doi.org/10.52589/IJMCE-VWINHURC

METHODOLOGY

Ordinary Portland cement

Ordinary Portland Cement (CEM II, grade 42.5N/mm²), weighing 150 kg, was procured locally and confirmed to satisfy Portland cement requirements by NIS 367 (1997) and NIS 368-2 (1990).

Lateritic soil

500kg of lateritic soil obtained from sample borrow pit adjacent to the Central Bank of Nigeria, situated on the New Iyin-Ekiti road in Ado Ekiti was utilized for the research. Prior to brick manufacture, the material was pulverized using a toothed belt machine following air drying to ensure complete moisture removal. A 75µm sieve was employed to filter the pulverized lateritic soil.

Pozzolans (Sawdust ash)

The 50kg of sawdust waste was obtained from a nearby sawmill in Ado-Ekiti. The samples were incinerated individually in metal drums to produce greyish ash. This calcination technology was chosen due to its cost-effectiveness and compliance with requisite criteria. Subsequent to cooling, the ashes were subjected to sieving with a No. 200 (75µm) BS sieve in accordance with BS 12 (1991). The blend was created utilizing the samples that were selected. Table 2 presents the chemical composition of sawdust ash.

Table 2: SDA chemical composition (47)

S/No	**1**	**2**	**3**	**4**	**5**	**6**	**7**	**8**
Compound (%)	CaO	SiO_2	Al_2O_3	MgO	Fe_2O_3	SO_3	Na_2O	K_2O
SDA	8.09	62.43	4.36	3.59	4.92	1.07	0.06	3.95

Water

Potable water was used in accordance with [33] and [48].

Design of Mix proportions

A design that combines aspects of a two-level factorial design and an incomplete block design is known as the Box-Behnken Design (BBD) [45]. While other factors remain at the central levels, a certain number of factors are processed through all conceivable combinations for the factorial design in each block. Usually, it features a few focus designs.

The mix ratio for the bricks employing SDA as pozzolans was produced using Design Expert software (version 11) and the Box-Behnken Design (BBD) of Response Surface Methodology (RSM). The parts were assembled into a Box-Behnken Design to create a random number of trial runs. Table 3 presents the variables discovered in the BBD experimental region, and Table 4 displays the recommended BBD experimental design. A graduated beaker was used to

Article DOI: 10.52589/IJMCE-VWINHURC
DOI URL: https://doi.org/10.52589/IJMCE-VWINHURC

measure the water, and a weighing scale was utilized to quantify each component using values from Table 3. The components were afterward mixed by hand until uniform pastes were formed.

Table 3: Factors input for Box-Behnken Design

Factors	Code	Unit	Level		
			Low (-1)	Standard (0)	High (+1)
Saw Dust Ash (SDA	A	%	0	2.5	5.0
Cement	B	%	0	2.5	5.0
Water Content (WC)	C	%	20.0	22.5	25.0

Table 4: The experimental design using Box-Behnken Design

SAMPLE ID	SDA (%)	CEMENT (%)	W/C (%)
V1	3.75	1.25	21.25
V2	0.00	5.00	20.00
V3	1.25	3.75	22.50
V4	1.25	3.75	21.25
V5	5.00	0.00	20.00
V6	0.00	5.00	25.00
V7	3.75	1.25	22.50
V8	1.25	3.75	23.75
V9	5.00	0.00	25.00
V10	3.75	1.25	23.75
V11	0.00	5.00	22.50
V12	2.50	2.50	22.50
V13	5.00	0.00	22.50
V14	2.50	2.50	23.75
V15	2.50	2.50	25.00

Article DOI: 10.52589/IJMCE-VWINHURC
DOI URL: https://doi.org/10.52589/IJMCE-VWINHURC

V16	2.50	2.50	21.25
V17	2.50	2.50	20.00

Note: V – Sample ID

Moulding of Bricks

The damp mixture was put into a greased mould of a locally built mechanical press machine that was made at the Federal Polytechnic, Ado Ekiti. A timber bedstead was positioned underneath the machine's casing to ensure that the crushed bricks were transferred efficiently. The damp mixture was put into the machine's casing using a shovel and compacted using a 20mm-diameter rod. The machine was then sealed and put through 25 seconds of mechanical vibration [31]. The newly formed brick was then extruded using a wooden pallet, carefully moved to a shelter, and covered with polyethylene to stop moisture loss and speed up the curing process.

Compressive Strength (CS) of samples

The specimens were cured and tested at intervals of 28, 56, 108, and 365 days, adhering to ASTM C67 [32]. Prior to positioning and aligning the specimen with the loading apparatus, the bearing surfaces of the supporting and bearing rollers were meticulously cleaned; loading was applied gradually and continuously until the dial ceased movement, at which point the maximum load was recorded [32]. The compressive strength *(CS)* values were determined by calculating the mean of six (6) specimens. Testing was performed using the electronically operated Seidner (*CS)* machine. Equation (1) illustrates the specimen's *(CS),* expressed in N/mm^2.

$$CS = P/A \quad (1)$$

where *CS* is compressive strength in N/mm^2, P is the load at failure, and A is the sample cross-sectional area.

Water Absorption (WA)

In accordance with [32], the *WA* test was conducted. The dehydrated weight of the item was recorded prior to its immersion in water at room temperature (29°C) for one day. The specimens were subsequently dusted for 10 minutes to remove any residual moisture, and the wet weight was recorded. Equation 2 was employed to derive the *WA*. Three specimens were analyzed for each combination to achieve a statistically meaningful average.

$$WA = (w1-w2)/w2 \times 100\%. \quad (2)$$

where water absorption, wet weight, and dry weight are *WA*, W1, and W2 of the specimen, respectively.

Abrasion resistance of the samples (Wire brush test)

The test was carried out in compliance with [46]. After weighing the test specimen, the weight was noted as w1. After that, the sample was placed for brushing on a horizontal work surface.

Article DOI: 10.52589/IJMCE-VWINHURC
DOI URL: https://doi.org/10.52589/IJMCE-VWINHURC

A wire brush with a 3 kg mass attached was used to brush the sample's surface; the brush was placed on the specimen so that the mass was applied vertically, as illustrated in Figure 2. A minute-long cycle of alternating forward and backward brushing was conducted until 60 cycles were finished. All extraneous material was removed from the specimen, which was then reweighed and reported as w2. The mass of detachable stuff relative to the starting weight of the brick was determined using equation (3).

Abrasion = (w1-w2)/w1×100% (3)

Figure 1: Wire Brush Test (Abrasion Measurement)

Impact resistance of the samples

The Impact test was performed in accordance with [33]. Three samples were analyzed for each blend to derive a reliable average. A apparatus with a 508g iron weight, conforming to ISO 7892 standards, was employed for the test. The sample's initial weight, referred to as w1, was documented. The upper arm of the device, which was elevated and fixed one meter above the base, was where the metallic mass was attached. The sample was positioned on the base plate, and the specimen fractured as the metal item descended freely onto it. The majority of the material was extracted, weighed, and recorded as w2. Equation 4 was employed to assess the brick's impact resistance relative to the starting sample's weight.

Impact= (w1-w2)/w1×100% (4)

Sulphate Attack

According to [34], two test media were prepared: a water bath and a sulphate bath with a 3% Na_2SO_4 solution. The samples were weighed first, then soaked in water for 80 days (one sample per medium), extracted, drained, and oven-dried for 42 hours at 71°C. After drying for two hours, the samples were brushed and weighed again to determine the weight losses in both media.

Microstructural Analysis

The brick samples were cured for 28, 56, 108, and 365 days were examined under a Scanning

Article DOI: 10.52589/IJMCE-VWINHURC
DOI URL: https://doi.org/10.52589/IJMCE-VWINHURC

International Journal of Mechanical and Civil Engineering (IJMCE)
ISSN: 2689-940X
Volume 9, Issue 1, 2026 (pp. 18-38)
www.abjournals.org

Electron Microscope (SEM). Samples are produced at dimensions of approximately 8x8 mm² and are coated with platinum before analysis. After being placed in the chamber of a scanning electron microscope, the coated samples are analyzed under vacuum conditions at a voltage of 20 kV using the JEOL-JSM 7600F. The scanning electron microscope employs a small external magnetic field on the objective lens. The device can magnify objects by a factor of 500 and functions within a range of 1 to 25 mm, among other capabilities.

RESULTS

Optimization Studies of the Parameters

All parameters of the study, including abrasion, compressive strength (CS), impact resistance, sulphate attack, and water absorption, were statistically analyzed using Design Expert software (version 11–DOEV11). The independent and dependent variables of the study were delineated. The values for each parameter employed in the optimization analysis are presented in Table 2. DOEv6 was utilized to assess the experimental data, calculate the predicted responses, and formulate the factorial regression model to identify the optimal conditions and optimization process. Correlation analysis and three-dimensional (3D) response surface graphs of the independent variable and each of the three dependent variables for all parameters were employed to ascertain the appropriate removal conditions. The method was refined using models initially developed in the response surface domain.

Water Absorption

For 28, 56, 108, and 365 days, respectively, the mix proportions with the lowest water absorption values are V13 (SDA – 5.00%, Cement – 0%, W/C – 20.00%), V10 (SDA – 3.75%, Cement – 1.25%, W/C – 23.75%), V2 (SDA – 0%, Cement – 5.00%, W/C – 20.00%), and V13 (SDA – 5.00%, Cement – 0%, W/C – 22.50%), according to Figure 5. For 28 and 56 days, the mix ratios V2 (SDA – 0%, Cement – 5.00%, and W/C – 20.00%) and V4 (SDA – 1.25%, Cement – 3.75%, and W/C – 21.25%) had the highest WA rates. The above water absorption rate values for the SDA-free brick samples (V2, V6, and V11) vary from 10% to 40%, 12% to 45%, 5% to 12%, and 5% to 10%, respectively, after 28, 56, 108, and 365 days. Samples with an SDA concentration of 1.25% (V3, V4, and V8) exhibit WA rates ranging from 20% to 35%, 25% to 35%, 15% to 30%, and 5% to 10% over intervals of 28, 56, 108, and 365 days, respectively. The water absorption values rate results of brick samples with 2.5% SDA content (V12, V14, V15, V16, and V17) varied from 20% to 30%, 15% to 40%, 15% to 30%, and 5% to 10% after 28, 56, 108, and 365 days, respectively (Figure 2). The SDA content of 3.75% (V1, V7, and V10) varied between -5% and 25%, 15% and 35%, 15% and 30%, and 5% and 10%, respectively, across 28, 56, 108, and 365 days. Brick samples with 5% SDA (V5, V9, and V13) had the water absorption rate values ranging from -10% to 20%, -20% to 20%, -20% to 15%, and 0% to 5% at 28, 56, 108, and 365 days respectively and surface area, as illustrated in Fig. 2.

Article DOI: 10.52589/IJMCE-VWINHURC
DOI URL: https://doi.org/10.52589/IJMCE-VWINHURC

Figure 2: Graph of SDA Bricks' Absorption of water

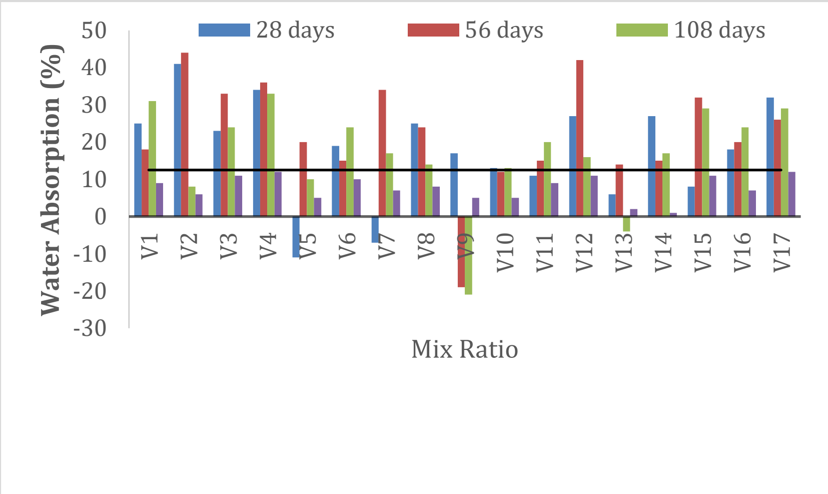

The bricks, including SDA exhibited enhanced resistance to water absorption as the curing age progressed; All bricks produced satisfied the requisite grade of 12.5% at 365 days, as per [38] SDA, concentrations ranging from 0 to 2.5% were used to achieve the desired WA resistance, which is comparable to cement. Samples without cement (i.e., pozzolans alone) exhibit the lowest resistance to water absorption as the curing age increases, whereas samples without pozzolans (i.e., Control) exhibit the maximum resistance. The findings were validated by [35] [36] and [37].

Abrasion resistance of SDA Bricks

Bricks manufactured using SDA were found to function well in terms of abrasion resistance, as all of the samples satisfy the less than 10% necessary criteria as stated by [38]. Abrasion values for 28 days are lowest for mix ratio V11 (SDA – 0%, Cement – 5.00%, and W/C – 22.50%), whereas for 56, 108, and 365 days (Fig. 3), the lowest abrasion values are found for mix ratio V2 (SDA – 0%, Cement – 5.00%, and W/C – 20.00%). The maximum abrasion values were found for 28 and 365 days with mix ratio V9 (SDA – 5.00%, Cement – 0%, and W/C – 25.00%) and 56 and 108 days with mix ratio V1 (SDA – 3.75%, Cement – 1.25%, and W/C – 21.25%). The abrasion values of brick samples without SDA (V2, V6, and V11) fluctuated between 1.0 and 2.0%, 0.7 and 1.0%, 0.5 and 2.0%, and 0.2 and 2.0% for 28, 56, 108, and 365 days, respectively. For those with 1.25% SDA content (V3, V4, and V8), the corresponding abrasion values were 2.0 to 5.0%, 1.0 to 3.0%, 2.0 to 4.0%, and 2.0 to 3.0%. The abrasion values of brick samples (V12, V14, V15, V16, and V17) with a 2.5% SDA concentration ranged from 2.0 to 6.0%, 1.5 to 4.0%, 3.0 to 5.0%, and 3.0 to 6.0%. The range of the 3.75% SDA content (V1, V7, and V10) was 2.0 to 4.5%, 3.0 to 9.0%, 5.0 to 8.0%, and 5.0 to 6% in that sequence. The abrasion values of brick samples with 5% SDA content (V5, V9, and V13) ranged between 2.0 and 7.0%, 3.0 and 5.0%, 5.0 and 7.0%, and 2.0 and 7.0% during 28, 56, 108, and 365 days, respectively.

Article DOI: 10.52589/IJMCE-VWINHURC
DOI URL: https://doi.org/10.52589/IJMCE-VWINHURC

Figure 3: Graph of SDA's Abrasion

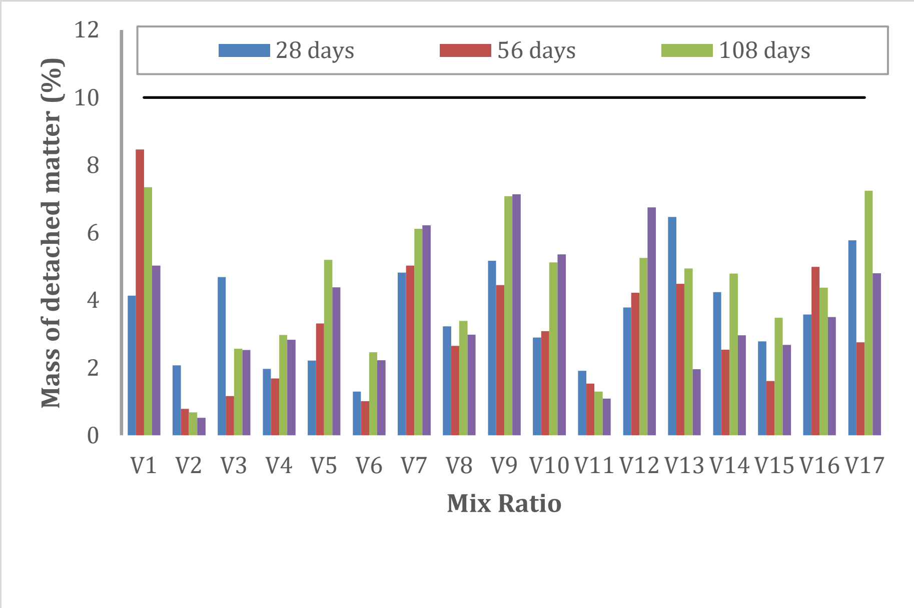

Most of the samples showed a rise in impact resistance as the curing ages for SDA grew, with the age approaching 365 days. Most of the samples of both pozzolans showed impact resistance of less than 10%, as needed by the [38] criterion at 365 days (Fig. 4).

Figure 4: Graph of impact with SDA as pozzolan

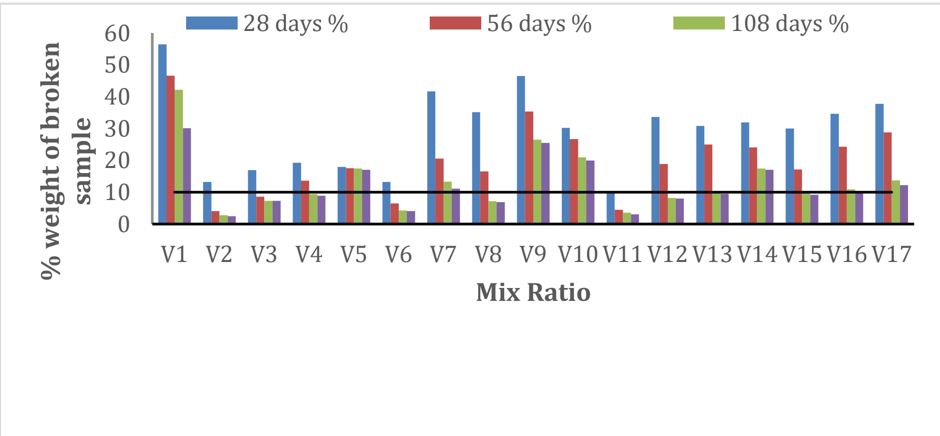

The mix ratio V11 (SDA – 0%, Cement – 5.00%, and W/C – 22.50%) has the lowest impact value at 28 days. The mix ratio V2 (SDA – 0%, Cement – 5.00%, and W/C – 20.00%) has the lowest impact value at 56, 108, and 365 days. The mix ratio V9 (SDA, 5.0% cement-0.0% and W/C-25.0% has the lowest impact value at 56, 108, and 365 days. The impact values for SDA-free brick samples (V2, V6, and V11) after 28, 56, 108, and 365 days are 8.0% to 13.0%, 2.5% to 7.5%, 2.0% to 5.0%, and 2.0% to 3.0%, respectively. For samples V3, V4, and V8, the impact values are 15.0% to 25.0%, 8.0% to 18.0%, 5.0% to 8.0%, and 5.0% to 6% in that sequence. The effect values for the brick samples with 2.5% SDA (V12, V14, V15, V16, and V17) were between 20.0% and 35.0%, 14.0% and 20.0%, 5.0%,15.0%, 5.0% and 10.0%. The SDA content of 3.75% (V1, V7, and V10) ranged from 30.0% to 45.0%, 18.0% to 35.0%,

Article DOI: 10.52589/IJMCE-VWINHURC
DOI URL: https://doi.org/10.52589/IJMCE-VWINHURC

10.0% to 28.0%, and 10.0% to 25.0%, respectively. The effect values for brick samples with 5% SDA (V5, V9, and V13) were between 15.0% and 40.0% at 28, 56, and 108 days and between 15.0% and 30.0% at 365 days.

Sulphate attack

Figure 5 shows that mix ratio V11 had the lowest sulphate attack value for 28 days, followed by mix ratio V15 (2.50% SDA, 2.50% Cement, and 25.00%) for 56 days, V1 (3.75% SDA, 1.25% Cement, and 21.25%) for 108 days, and mix ratio V6 (0% SDA, 5.00% Cement, and 25.00%) for 365 days. It took 108 days for the SDA pozzolan V5, V9, and V13 to become resistant to sulphate attack. Bricks fell apart in water because V5, V9, and V13 are mix proportions that have 100% pozzolan and no cement, which stops hydration. The sulphate attack values for brick samples from V2, V6, and V11 that do not have SDA are 15.0 to 20.0%, 15.0 to 20.0%, 15.0 to 20.0%, and 0 to 5.0% for 28, 56, 108, and 365 days. The sulphate attack values for V3, V4, and V8, which have an SDA content of 1.25%, are 18.0 to 20.0%, 15.0 to 25.0%, 8.0 to 12.0%, and 0 to 8.0%. The sulphate attack values for brick samples with a 2.5% SDA content (V12, V14, V15, V16, and V17) were between 0 and 20.0%, 10.0 and 20.0%, 10.0 and 15.0%, and 5.0 and 10.0%. The ranges were 12.0 to 25.0%, 15.0 to 18.0%, 5.0 to 8.0%, 2.0 to 5.0%, and so on with an SDA content of 3.75% (V1, V7, and V10). The sulphate attack values for brick samples with 5% SDA content (V5, V9, and V13) were between 35.0% and 45.0% for 365 days and between 95.0% and 100.0% for 28, 56, and 108 days, respectively.

Brick samples that don't include pozzolan such as V2, V6, and V11) are normally the most resistant to sulphate attack. On the other hand, samples with the most pozzolanic concentrations are the least resistant. In other words, resistance to sulphate attack gets better when the concentration of pozzolanic material goes down. This might happen because there wasn't enough cementation at high pozzolanic concentrations, as [38] showed. The bricks made with SDA were better able to resist sulphate attacks because they had more alumina and ferric oxides in them. However, most of the pozzolan samples showed less than 10% sulphate attack resistance at 365 days, which is what the [39] standard calls for. Equation 5 depicts the sulphate attack equation as proposed by [40].

$$3[CaSO4.2H_2O] + 3CaO \cdot Al_2O_3 + 26H_2O \rightarrow 3CaO \cdot Al_2O_3 \cdot 3CaSO_4 \cdot 32H_2O \quad [5]$$

Figure 5: Graph of sulphate attack with SDA as pozzolan

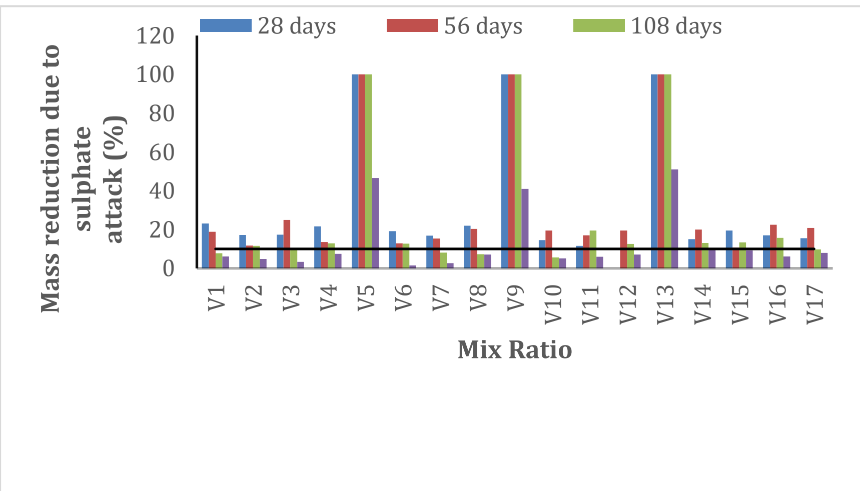

Article DOI: 10.52589/IJMCE-VWINHURC
DOI URL: https://doi.org/10.52589/IJMCE-VWINHURC

Microstructural Characteristics

Figs. 6a-6d show the microstructural properties of the SDA-Cement stabilized lateritic soil that was cured for 28, 56, 108, and 365 days. The SEM micrographs showed that the ideal SDA levels resulted in better pozzolanic activity, stronger particle bonding, and smaller pore gaps. The SEM micrographs reveal that the pozzolanic activity has gone up. This means that calcium hydroxide in the soil mixed with silica and alumina from sawdust ash to make more calcium silicate hydrate (C–S–H) and other cementitious compounds. The reaction products fill up gaps and make it easier for soil particles to stick together, which improves interparticle bonding. Better bonding makes the matrix denser and more cohesive, which makes the bricks stronger against applied loads and increases their compressive strength. The SEM photos show that the pore spaces have gotten smaller, which means that there are fewer and smaller capillary routes that water can get through. Densification makes it harder for moisture to get in and lowers the bricks' total porosity. The lower level of interconnected porosity means that the bricks absorb less water, which makes them last longer and better able to withstand the weather.

According to [41], the fineness of the pozzolan used is what gives pozzolan-substituted mortar or brick the maximum CS. The best pozzolan fineness can help you get the most CSs. The fineness of SDA in this study is very important for the growth of CS, resistance to abrasion, and resistance to sulphate attack in the brick-making process. As the number of curing days goes up, the number of pores goes down. This makes the WA go down and the CS, abrasion, and sulphate attack resistance go up. Researchers found that the microstructure of the SDA-Cement stabilized soil samples looked a lot like what is illustrated in Figure 6. On the other hand, samples that were cured for 28 and 108 days had gel-like coatings that were evenly spread out and looked more white than grey throughout their grey-like matrix. The white gel-like covering on the surface is caused by calcium silicate hydrates (C-S-H) gel, and the greyish matrix is caused by calcium aluminate silicate hydrates (C-A-S-H) gel. This structure has been seen in earlier research [42] and [43]. The development of the C-A-S-H structure in the SDA-cement-stabilized soil samples may result from the significant amount of aluminium inherent in the standard composition of SDA. Also, after 108 days of curing, soil-cement clusters are well-established, and you can clearly see the hydration products (C-S-H). This is because cementitious chemicals like C-S-H and C-A-S-H have been rising for a long time. Also, as plate 4.2 shows, the number of pores grows during the first stages of hydration. However, as curing goes on for a longer time, the number of pores shrinks, possibly because cementitious materials cover the pores.

Article DOI: 10.52589/IJMCE-VWINHURC
DOI URL: https://doi.org/10.52589/IJMCE-VWINHURC

Figure 6: SDA-Cement stabilized brick SEM image cured for (A) 28 days, (B) 56 days, (C) 108 days and (D) 365 days.

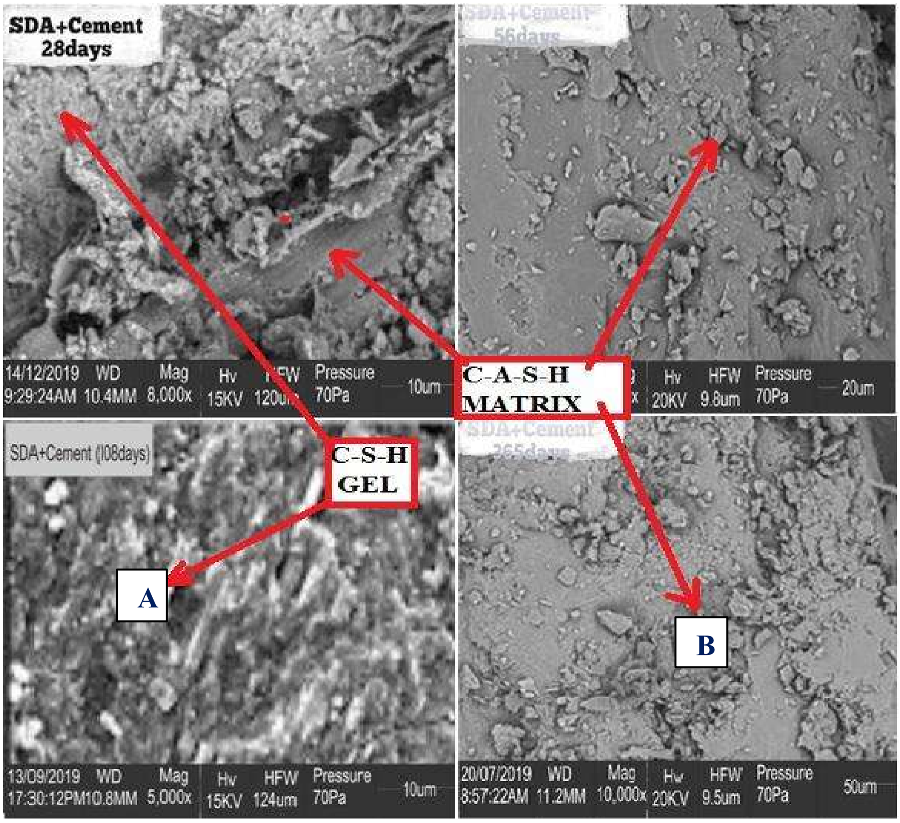

Optimization Characteristics

Figs. 7–10 illustrate the 3D response surface plots as functions of the three parameters for models of the properties of SDA bricks. The response surface plot was used to look at the non-linear interaction between factors. It demonstrates how the CS, WA, abrasion, impact, and sulphate attack on the interlocking stabilized bricks is affected by the amount of cement, pozzolans (SDA), and water (WC). The charts illustrate that the different effects of cement don't seem to matter much.

The chosen response surface model predictions were used to check the models. The red area in the figures shows the main reaction zone, the green area shows the feasible reaction zone (which means that a reaction can happen there even though there are impurities), and the blue area shows the cold zone (which means that a peak reaction is likely to happen there, but the chance is very low). The high edges show that the reaction is quite popular in that location. The saddle shape of all the models shows that all three were participating in the process, but two were more important at any given time. Table 5 shows how the plots' features backed up the models' polynomial nature.

Article DOI: 10.52589/IJMCE-VWINHURC
DOI URL: https://doi.org/10.52589/IJMCE-VWINHURC

Table 5: Summary of the Design of the Factors and Responses

Factor	Response	Units	Analysis	Transform	Model
PM (%)	28	days	Polynomial	None	Cubic
	56	days	Polynomial	None	Cubic
	108	days	Polynomial	None	Cubic
	365	days	Polynomial	None	Cubic
Cement (%)	28	days	Polynomial	None	Cubic
	56	days	Polynomial	None	Cubic
	108	days	Polynomial	None	Cubic
	365	days	Polynomial	None	Cubic
WC (%)	28	days	Polynomial	None	Cubic
	56	days	Polynomial	None	Cubic
	108	days	Polynomial	None	Cubic
	365	days	Polynomial	None	Cubic

Figure 7: Response surface plot showing the relationship between cement and SDA on all investigated properties of interlocked stabilized bricks at 28days of curing.

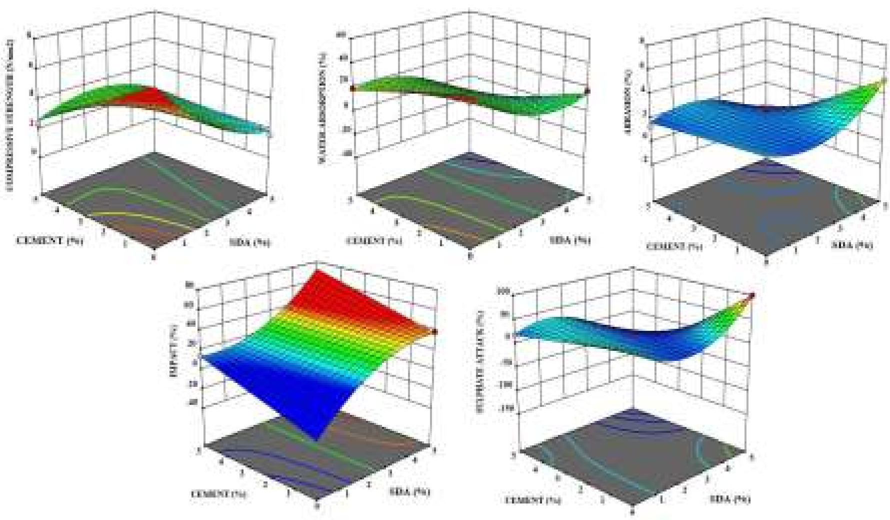

Article DOI: 10.52589/IJMCE-VWINHURC
DOI URL: https://doi.org/10.52589/IJMCE-VWINHURC

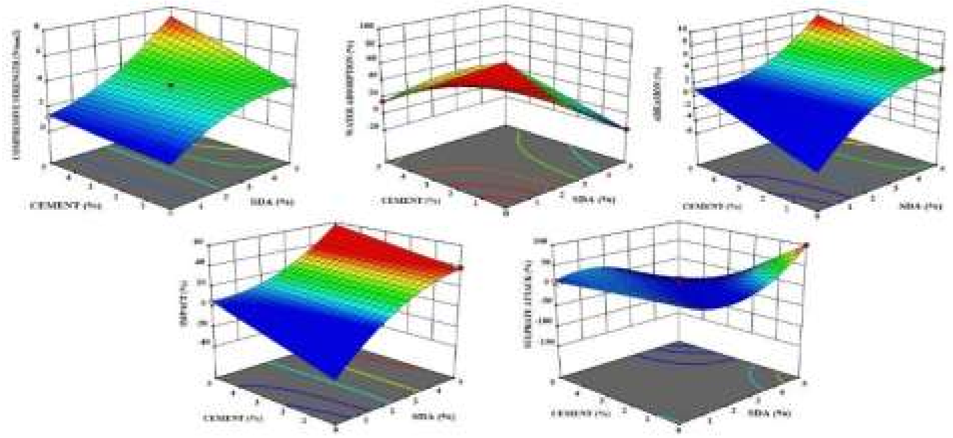

Figure 8: After 56 days of curing, the response surface plot illustrates the link between cement and SDA on all examined parameters of interlocked stabilized bricks.

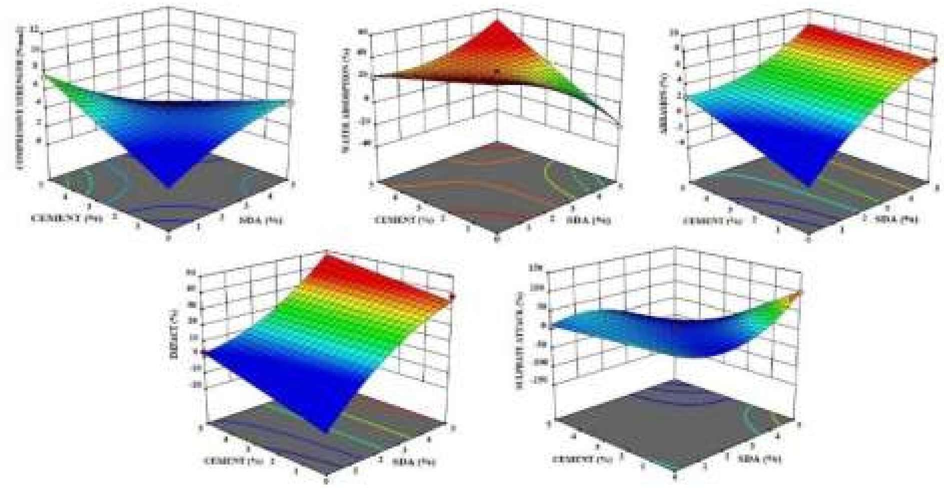

Figure 9: At 108 days of curing, a response surface plot illustrating the impact of cement and SDA on all examined parameters of interlocked stabilized bricks.

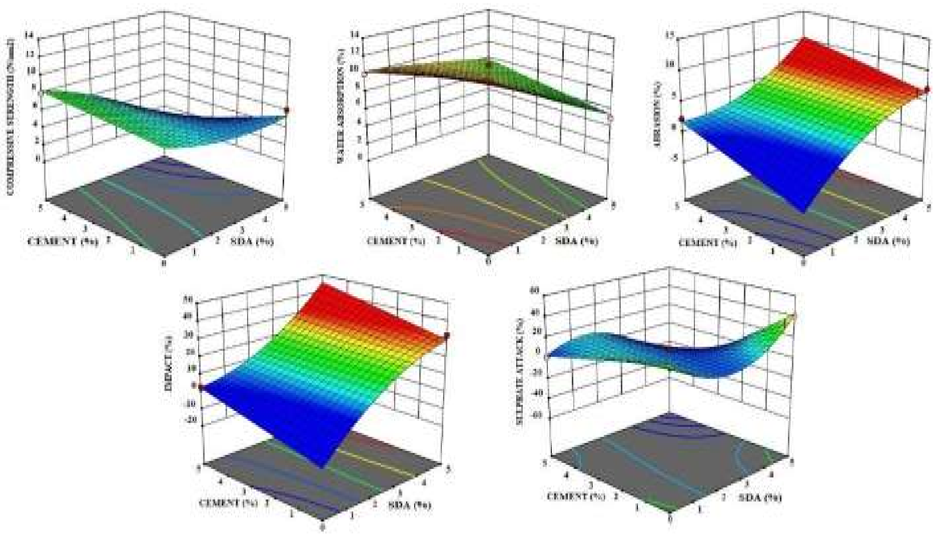

Article DOI: 10.52589/IJMCE-VWINHURC
DOI URL: https://doi.org/10.52589/IJMCE-VWINHURC

Figure 10: At 365 days of curing, a response surface plot illustrating the impact of cement and SDA on all examined parameters of interlocked stabilized bricks is displayed.

Table 6 shows that the response surface models used SDA and the constraint values to find the design point solutions (optimized numerical solutions) for the bricks. The optimization solution that was chosen was 25% water, 0.047% cement, and 4.571% SDA. As the bricks got older, this solution helped the CS grow. The CS values varied greatly, from 2.028 N/mm^2 (28 days) to 5.186 N/mm^2 (365 days). The values of WA, abrasion, impact, and sulphate attack went down as the curing age went up. The ranges for these values were 12.328–6.106%, 6.537–4.067%, 18.080–8.598%, and 25.369–9.853%. As the curing age went up, these SDA solutions often made CS, abrasion resistance, impact resistance, and sulphate attack resistance better.

Table 6: Numerical solutions that are optimized for response surface models Sawdust Ash

S	SDA (%)	CEMENT (%)	WC (%)	DAYS			
				28	56	108	356
CS (N/mm^2)	4.571	4.7	25	2.028	3.817	4.772	5.186
Water Absorption (%)				12.328	12.099	8.703	6.106
Abrasion (%)				6.537	6.46	4.327	4.067
Impact (%)				18.08	16.202	13.074	8.598
Sulphate Attack (%)				25.369	16.775	15.576	9.853

CS: Compressive strength

CONCLUSIONS

The research results yield the subsequent conclusions:

i. The lateritic soil was classified as silty clay (A-7-6 with more than 35% passing through a No. 200 screen), whereas the sawdust ash (SDA) was classified as a Class F pozzolan, with high quantities of silica, calcium, alumina, and ferric oxides.

ii. Cement-SDA stabilized bricks satisfied the minimal compressive strength requirements, and they worked best when 0–2.5% of the SDA was replaced.

iii. SEM micrographs showed that the small SDA particles helped the matrix become denser, made it less porous, and made the bonds between particles stronger. This improved the engineering qualities of the stabilized bricks over time.

iv. Curing improved the durability by making it less likely to absorb water, making it more resistant to abrasion (≤10%), and making it more resistant to sulphate, especially at

Article DOI: 10.52589/IJMCE-VWINHURC
DOI URL: https://doi.org/10.52589/IJMCE-VWINHURC

lower SDA levels. SEM research shows that the improved mechanical and durability qualities are attributable to pozzolanic reactions caused by the high silica content and better particle packing from the tiny SDA particles.

v. SDA-stabilized bricks are good for both the foundation and the superstructure. They are a long-lasting choice that uses waste while keeping the construction strong.

Funding: None.

Ethics, Consent to Participate and Consent to Publish declarations: Every author consented to the manuscript's publication.

Data availability: The manuscript contains all the research data.

Competing interest: not applicable.

Acknowledgments: The authors would like to thank all of the laboratory technologists at Ekiti State University and the Federal Polytechnic's Civil Engineering departments in Ado Ekiti.

REFERENCES

[1] Osunade, James A. (2002). Effect of replacement of lateritic soils with granite fines on the compressive and tensile strengths of laterized concrete. *Building and Environment, 37*(5), 491–496. https://doi.org/10.1016/S0360-1323(01)00049-6

[2] Naderpour, Hamid, Rafiean, Ali H., & Fakharian, Parisa. (2018). Compressive strength prediction of environmentally friendly concrete using artificial neural networks. *Journal of Building Engineering, 16*, 213–219. https://doi.org/10.1016/j.jobe.2017.12.012

[3] Kennedy, Chinedu O., Van, Daniel B., Ubachukwu, Obinna, et al. (2019). Recycling and reuse of solid wastes: A hub for eco-friendly, efficient and sustainable soil, concrete, wastewater and pavement reengineering. *International Journal of Low Carbon Technologies, 1*, 1–10.

[4] Olonade, Kayode A. (2013). Economy of RHA (Rice Husk Ash) in concrete for low-cost housing delivery in Nigeria. *Journal of Civil Engineering and Architecture, 7*(11), 1464–1470.

[5] Ogbonna, Chukwuemeka, Mbadike, Emeka M., & Alaneme, Godwin U. (2020). Effects of cassava-peel-ash on mechanical properties of concrete. *Umudike Journal of Engineering and Technology, 6*(2), 61–75.

[6] Frías, Miguel, Rodríguez, Oscar, Sanchez de Rojas, María I., Villar-Cociña, Ernesto, Rodrigues, Maria S., & Savastano Junior, Holmer. (2017). Advances on the development of ternary cements elaborated with biomass ashes coming from different activation processes. *Construction and Building Materials, 136*, 73–80. https://doi.org/10.1016/j.conbuildmat.2017.01.034

[7] Ayangade, James A., Olusola, Kolapo O., Ikpo, Innocent J., & Ata, Oladipo. (2004). Effect of granite dust on the performance characteristics of Kernelrazzo floor finish. *Building and Environment, 39*(10), 1207–1212.

[8] Malik, Mohammad I., Jan, Syed R., Peer, Javid A., Nazir, Shafiq A., & Mohammad, Khalid F. (2015). Partial replacement of cement by sawdust ash in concrete: A sustainable approach. *International Journal of Engineering Research and Development, 11*(2), 48–53.

[9] Antiohos, Stavros, Maganari, Konstantina, & Tsimas, Stavros. (2005). Evaluation of blends of high and low calcium ashes for use as supplementary cementing materials. *Cement and Concrete Composites, 27*(3), 349–356. https://doi.org/10.1016/j.cemconcomp.2004.02.006
[10] Mwango, Andrew, & Kambole, Chanda. (2019). Engineering characteristics and potential increased utilisation of sawdust composites in construction—A review. *Journal of Building Construction and Planning Research, 7*(1), 59–88.
[11] Coutinho, Joaquim S. (2003). The combined benefits of CPF and RHA in improving the durability of concrete structures. *Cement and Concrete Composites, 25*(1), 51–59. https://doi.org/10.1016/S0958-9465(01)00057-9
[12] Chowdhury, Suman, Mishra, Manish, & Suganya, Oviya. (2015). The incorporation of wood waste ash as a partial cement replacement material for making structural grade concrete: An overview. *Ain Shams Engineering Journal, 6*(2), 429–437. https://doi.org/10.1016/j.asej.2014.11.005
[13] Bratkovich, Stephen, Howe, James, Bowyer, Jim, Pepke, Eric, Frank, Mark, & Fernholz, Kathryn. (2014). Municipal solid waste (MSW) and construction and demolition (C&D) wood waste generation and recovery in the United States. *Dovetail Partners Report, 1*, 1–16.
[14] Röder, Michael, & Thornley, Patricia. (2018). Waste wood as bioenergy feedstock: Climate change impacts and related emission uncertainties from waste wood-based energy systems in the UK. *Waste Management, 74*, 241–252. https://doi.org/10.1016/j.wasman.2018.01.018
[15] Brown, Michael, & Kearley, Victoria. (2009). Role of wood waste as source of biomass fuel in the UK. *Energy Materials, 4*(3), 162–165.
[16] Cheah, Chee Ban, & Ramli, Mahyuddin. (2013). The engineering properties of high-performance concrete with HCWADSF supplementary binder. *Construction and Building Materials, 40*, 93–103. https://doi.org/10.1016/j.conbuildmat.2012.09.103
[17] Obilade, Isaac O. (2014). Use of sawdust ash as partial replacement for cement in concrete. *International Journal of Engineering Science Invention, 3*(8), 36–40.
[18] Kashyap, Rakesh, Chaudhary, Manju, & Sen, Ankit. (2015). Effect of partial replacement of cement by rice husk ash in concrete. *International Journal of Scientific Research, 4*(5), 1572–1574.
[19] Ganesah, Krishnan, Rajagopal, Karthik, Thangavel, Kumar, Selvaraj, Ramesh, & Saraswathi, Vasantha. (2004). Rice husk ash – A versatile supplementary cementitious material. *Indian Concrete Institute Journal, 78*(11), 29–34.
[20] Chen, Yan, Saqib, Muhammad, Shahzada, Khurram, Aizaz, Muhammad, & Gul, Asif. (2025). Assessment of mechanical properties and durability of compressed mud bricks stabilized with stone dust, wheat straw, and cement. *Scientific Reports, 15*(1), 1950. https://doi.org/10.1038/s41598-025-86473-2
[21] Iorliam, Yandev A., Tile, Joseph T., & Ukya, James T. (2023). Effect of sawdust ash and rice husk ash on some geotechnical properties of Makurdi burnt clay bricks. *FUOYE Journal of Engineering and Technology, 8*(2). https://doi.org/10.46792/fuoyejet.v8i2.960
[22] Dhimal, Sushil, & Gautam, Gopal. (2024). Laboratory investigation on improving strength of weak subgrade soil using sawdust ash with stone dust. *Journal of Science and Technology, 4*(1), 53–57. https://doi.org/10.3126/jost.v4i1.74566
[23] Kumar, Sandeep, Chopra, Anil, & Ha, Zubair U. (2023). Sustainable geopolymer bricks: Optimizing fly ash, rice husk ash, and marble dust composites. *Preprint, Research Square*. https://doi.org/10.21203/rs.3.rs-3621641/v1

[24] Garg, Ankit, & Sharma, Pradeep K. (2022). Cost effective light weight concrete with sawdust and brick ballast. *Journal of Physics: Conference Series, 2267*(1), 012110. https://doi.org/10.1088/1742-6596/2267/1/012110

[25] Iro, Uzoma I., Alaneme, George U., Milad, Abdalrhman, Olaiya, Bamidele C., Otu, Obeten N., Isu, Edward U., & Amuzie, Magnus N. (2022). Optimization and simulation of sawdust ash concrete using extreme vertex design method. *Advances in Materials Science and Engineering, 2022*, Article ID 5082139, 22 pages. https://doi.org/10.1155/2022/5082139

[26] Awolusi, Temitope F., Sojobi, Ayodele O., Oguntayo, David O., Akinkurolere, Olumide O., & Orogbade, Babatunde O. (2021). Effects of calcined clay, sawdust ash and chemical admixtures on strength and properties of concrete for pavement and flooring applications using Taguchi approach. *Case Studies in Construction Materials, 15*, e00568. https://doi.org/10.1016/j.cscm.2021.e00568

[27] Singh, Rajesh, & Patel, Manish. (2025). Mechanical, durability, and microstructural characteristics of rice straw-ash-based clay bricks: A sustainable approach to utilize biomass-based power plant waste. *Journal of Material Cycles and Waste Management, 27*, 170–192. https://doi.org/10.1007/s10163-024-02101-7

[28] Adeleke, Ayodeji A., Ikubanni, Peter P., Odusote, Joshua K., et al. (2023). Influence of sawdust ash on the microstructural and physicomechanical properties of stir-cast Al6063/SDA matrix composite. *International Journal of Advanced Manufacturing Technology, 127*(5–6), 2523–2536. https://doi.org/10.1007/s00170-023-11700-x

[29] Malik, Mohammad I., Jan, Syed R., Peer, Junaid A., Nazir, Syed A., & Mohammad, Khubbab F. (2015). Partial replacement of cement by saw dust ash in concrete: A sustainable approach. *International Journal of Engineering Research and Development, 11*(2), 48–53. Retrieved from http://www.iensci.org

[30] Omoregie, Augustine. (2012). Impact of vibration time on compressive strength of hardened sandcrete building blocks. *Buildings, 2*(2), 153–172. https://doi.org/10.3390/buildings2020153

[31] American Society for Testing and Materials. (2020). *ASTM C67: Testing of bricks and structural clay tiles*. ASTM International. West Conshohocken, PA: Philadelphia.

[32] American Society for Testing and Materials. (2013). *ASTM C1747/C1747M-13: Standard test method for determining potential resistance to degradation of pervious concrete by impact and abrasion*. ASTM International. West Conshohocken, PA: Philadelphia.

[33] American Society for Testing and Materials. (2015). *ASTM C1012/C1012M: Guidelines for sulfate resistance for mortar*. ASTM International. West Conshohocken, PA: Philadelphia.

[34] Agbede, Isaac O., & Joel, Michael. (2011). Effect of rice husk ash (RHA) on the properties of Ibaji burnt clay bricks. *American Journal of Scientific and Industrial Research, 2*(4), 674–677.

[35] Fernando, Priyan R. (2017). Experimental investigation of the effect of fired clay brick on partial replacement of rice husk ash (RHA). *Advances in Recycling and Waste Management, 2*(1), 1–4.

[36] Ismail, Norazian, Salleh, Noraini, Yusof, Noor F. M., Jamellodin, Zulkifli, & Jaafar, Mohd F. M. (2017). Strength, water absorption and thermal comfort of mortar bricks containing crushed ceramic waste. *Jurnal Teknologi, 79*(7), 167–173.

[37] Adetoro, Ayodele E., & Faluyi, Samuel O. (2015). Potentials of non-cementitious additives for stabilization of Oye local government area soil, Ekiti State, Nigeria. *International Journal of Scientific Research in Knowledge, 3*(1), 288–296.

Article DOI: 10.52589/IJMCE-VWINHURC
DOI URL: https://doi.org/10.52589/IJMCE-VWINHURC

[38] Nigeria Building and Road Research Institute (NBRRI). (2011). *NBRRI materials research and testing manual*. Abuja, Nigeria: Federal Ministry of Science and Technology.
[39] Abubakar, Bashir H., Wan Ibrahim, Mohd H., & Megat Johari, Mohd A. (2010). A review: Durability of fired clay brick masonry wall due to salt attack. *International Journal of Integrated Engineering (Civil and Environmental Engineering Issue), 35*, 1–10.
[40] Rashad, Alaa M., Seleem, Hossam E. H., & Shaheen, Ahmed F. (2014). Effect of silica fume and slag on compressive strength and abrasion resistance of HVFA concrete. *International Journal of Concrete Structures and Materials, 8*(1), 69–81.
[41] Karim, Mohd, Hashim, Hamzah, Abdulrazak, Hassan, & Yusoff, Siti. (2017). Characterization of palm oil clinker powder for utilization in cement-based applications. *Construction and Building Materials, 135*, 21–29. https://doi.org/10.1016/j.conbuildmat.2016.12.158
[42] Puertas, Fernando, Palacios, Marta, Manzano, Hernán, Dolado, Juan S., Rico, Antonio, & Rodriguez, Javier. (2011). A model for the C-A-S-H gel found in alkali-activated slag cements. *Journal of the European Ceramic Society, 31*(12), 2043–2056
[43] Raul, Francisco, Ana, Isabel S., & Jaime, Carlos. (2016). Formation of C-A-S-H phases from the interaction between concrete or cement and bentonite. *Clay Minerals, 51*(14), 223–235.
[44] Wang, Jian, & Wan, Weiguo. (2009). Experimental design methods for fermentative hydrogen production: A review. *International Journal of Hydrogen Energy, 34*(1), 235–244. https://doi.org/10.1016/j.ijhydene.2008.10.008
[45] American Society for Testing and Materials. (2010). *ASTM C944-99: Standard test method for abrasion resistance of concrete or mortar surfaces by the rotating-cutter method*. ASTM International. West Conshohocken, PA: Philadelphia.
[46] Raheem, Abiodun A., & Ige, Ayodele I. (2019). Chemical composition and physicomechanical characteristics of sawdust ash blended cement. *Journal of Building Engineering, 21*, 404–408. https://doi.org/10.1016/j.jobe.2018.10.014
[47] British Standards Institution. (1991). *BS 12:1991 Specification for Portland cement*. London: BSI. https://doi.org/10.3403/00256361
[48] WHO (2017). The Guidelines for Drinking-Water Qualities (GDWQ), 4th Edition, WHO press, Geneva, Switzerland. 113 - 180

Article DOI: 10.52589/IJMCE-VWINHURC
DOI URL: https://doi.org/10.52589/IJMCE-VWINHURC